ACS Macro Letters

Letter

pubs.acs.org/macroletters

Diffusion of Entangled Rod−Coil Block Copolymers

Muzhou Wang,[†] Alfredo Alexander-Katz,[‡] and Bradley D. Olsen*,[†]

[†]Department of Chemical Engineering, Massachusetts Institute of Technology, Cambridge, Massachusetts 02139, United States

[‡]Department of Materials Science and Engineering, Massachusetts Institute of Technology, Cambridge, Massachusetts 02139, United States

Supporting Information

ABSTRACT: The diffusion of entangled rod−coil block copolymers is investigated by molecular dynamics (MD) simulations, and theories are introduced that describe the observed features and underlying physics. The reptation of rod−coil block copolymers is dominated by the mismatch between the curvature of the rod and coil entanglement tubes, which results in dramatically slower diffusion of rod−coils compared to the rod and coil homopolymers. For small rods, a local curvature-dependent free energy penalty results in a rough energy surface inside the entanglement tube, causing diffusivity to decrease with rod length. For large rods, rotational hindrances on the rod dominate, causing the coil block to relax by an arm retraction mechanism and diffusivity to decrease exponentially with coil size.

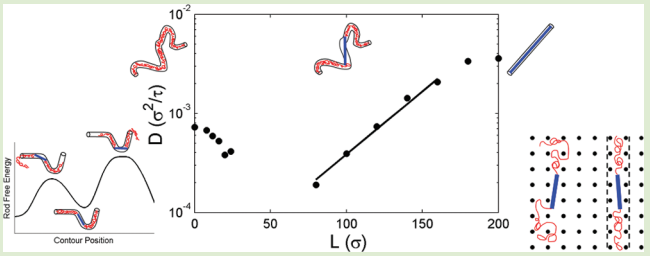

Rod−coil block copolymers have attracted extensive interest as functional nanostructured materials for organic electronics[1,2] and biomaterials.[2−4] The self-assembly behavior of these materials is fundamentally different from coil−coil block copolymers due to the mismatch between rod and coil chain topology and anisotropic interactions between the rod blocks.[2,5−7] Although the equilibrium thermodynamics of rod−coil block copolymers continues to be widely investigated, a fundamental knowledge of dynamics that is necessary for understanding diffusion, mechanics, processing, and the kinetics of self-assembly is lacking. These dynamic phenomena have only been explored in a few isolated studies. Rheological measurements have been used to identify order−disorder transitions[8,9] and to measure intrinsic viscosities.[10] Borsali et al. also provided analytical expressions for dynamic structure factors in dilute solution.[11] Further investigations are necessary to provide fundamental insight into the dynamics of these important polymer systems.

The dynamics of rod−coil block copolymers in the entangled regime is interesting both scientifically and technologically because the dynamics of rod polymers depart significantly from those of coil polymers, which dramatically affects the processing and self-assembly of materials in the melt. For coil polymers, reptation theories and experimental evidence have shown that diffusivity scales as $D \sim M^{-2.3}$ and end-to-end relaxation time scales as $\tau_r \sim M^{3.4}$.[12−14] For rod polymers, similar Doi−Edwards theories predict that diffusivity scales as $D \sim M^{-1}$ and end-to-end (rotational) relaxation time scales as $\tau_r \sim M^{9}$.[13,15] Though experimental evidence has shown that finite rod diameter, flexibility, and hydrodynamic interactions lead to modified scalings ($D \sim M^{-1.8}$, $\tau_r \sim M^{7-9}$),[16−18] the nature of dynamic entanglement is fundamentally different between rods and coils, leading to faster translational diffusion in rods but slower end-to-end relaxation due to their greater spatial extent.

In this Letter, the differences between rod and coil reptation are demonstrated to combine nonlinearly in rod−coil block copolymers to produce a regime of dynamic arrest, where diffusion is much slower than rod or coil homopolymers of the same total degree of polymerization. This effect is investigated using tracer diffusion of coil−rod−coil triblock copolymers in entangled coil homopolymer melts. Coil−rod−coil triblocks have been widely studied for their self-assembly behavior,[2,7,19] and they are well-suited for this initial study because both ends of the molecule relax according to the known theories of coil reptation. The use of coil homopolymers provides a well-studied entangling matrix that further capitalizes upon existing reptation knowledge. Molecular dynamics (MD) simulations are used to characterize the regime of dynamic arrest, and analytical theories are developed in both the small and large rod fraction limits to describe the observed diffusion. These theories provide a firm basis for considering more complex dynamic processes in rod−coil block copolymers such as melt diffusion and self-assembly kinetics.

In the small rod limit where the rod length is comparable to the entanglement length $L \sim a$, coil−rod−coil triblock tracer diffusion can be directly simulated by MD using minor modifications to the Kremer−Grest model[20] (details in Supporting Information). Rodlike behavior was enforced on a portion of the polymer molecule by a stiff three-bead bending potential $U_\theta = 1000\varepsilon(1 - \cos\theta)$, where ε is the characteristic energy. To simulate tracer diffusion, coil−rod−coils of $N = 200$

Received: March 17, 2012
Accepted: April 23, 2012
Published: May 16, 2012

or $N = 300$ beads with varying rod lengths were equilibrated in entangled coil polymer melts of $N = 1000$ beads. Matrix chains were large to suppress constraint release on the time scale of tracer disengagement, and the density of tracers was $\nu < L^{-3}$ (L is rod length) to minimize rod−rod interactions. Entanglement lengths reported in the literature at these parameters varied from $N_e = 35$[20] to $N_e = 85$,[21] so the tracers used in this study were moderately entangled. Mean squared displacements (MSD's) were measured for 760 tracers under each condition. A subdiffusive regime was observed at short times as predicted by reptation theory for coil homopolymers,[13] and diffusivity was measured using the slope of MSD in the linear Fickian regime.

These simulations show that, at a constant total molecular weight, the diffusivity of triblocks significantly slows with increasing rod length (Figure 1), indicating that the dynamics

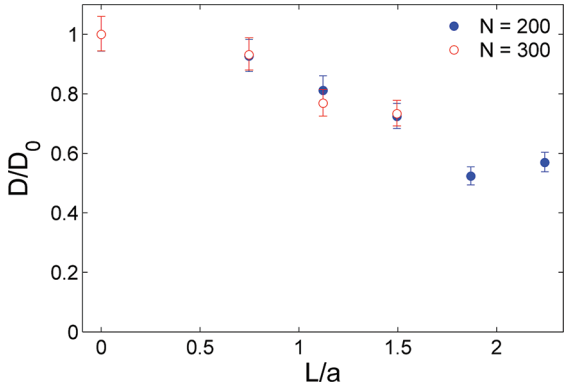

Figure 1. Diffusivities of coil−rod−coil triblocks of various lengths, normalized against the diffusivity of a coil homopolymer of the same size. Data are given for a total size of 200 monomers (closed circles) and 300 monomers (open circles), with $a = 10.7\sigma$ as estimated from the literature.[22,23] $N = 300$ was only simulated up to $L = 16\sigma$ due to limited computational time. The error bars depict 95% confidence intervals.

of rod−coil block copolymers is hindered as the rod approaches the entanglement length of the coil homopolymer matrix ($L \sim a$). Since rod polymers reptate faster than coil polymers, the unexpected slowing with increasing rod length indicates the presence of new physics in this system. The ratio of triblock to coil homopolymer diffusivity is only a function of the rod length and independent of the total tracer size, suggesting that the slowed diffusion is caused by an interaction between the rods and the surrounding entangled environment.

The unexpected slowing of coil−rod−coil triblock diffusion may be explained by a modified reptation theory where diffusion is slowed because the presence of the rigid rod block is entropically unfavored in the naturally curved sections of the coil block's entanglement tube. We refer to this unfavorability as *curvature mismatch* (CM). In the small rod limit, the coil−rod−coil tracer generates a new tube solely by exploring its surrounding space with its two coil ends. The observed diffusional slowing suggests that short rods reptating through this tube experience free energy barriers that hinder motion, and the size of these barriers increase monotonically with increasing rod length. While for sufficiently long rods these barriers will result in a transition from reptation to alternative diffusion mechanisms, for short rods the effect of the rod may be considered as a perturbation to coil polymer reptation, where the entanglement tube is defined by the coil polymer end blocks.

The presence of the rod and the associated CM effect can be parametrized by a free energy penalty: rods in a relatively straight section of the entanglement tube result in a low penalty associated with CM, while rods in curved sections produce a high CM energy (Figure 2a). Since the tube's curvature is a

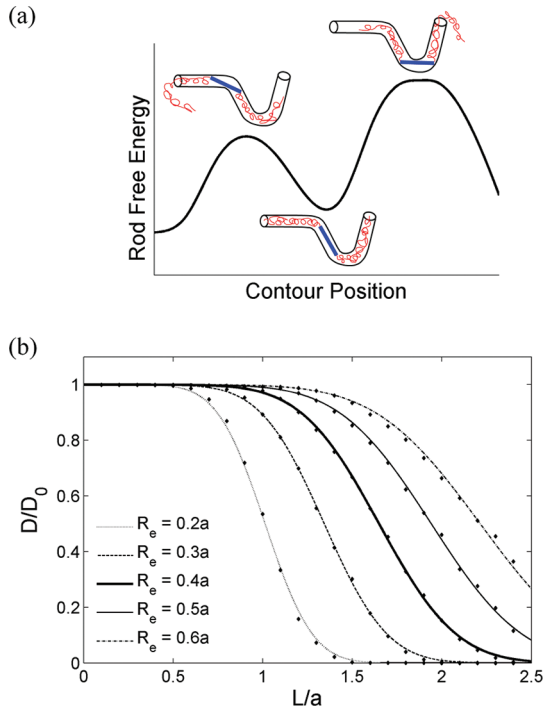

Figure 2. (a) The effect of curvature mismatch in the short rod limit. Rods in curved sections of an entanglement tube are entropically unfavored, resulting in a free energy penalty. (b) Predicted diffusivity vs rod length at various entanglement radii, normalized against coil homopolymer diffusivity. The small dots are from the Monte Carlo simulations, and the lines are empirical fits to an error function. Using $a \approx 10.7\sigma$ and $R_e \approx 4\sigma$ as estimated in the literature for Kremer−Grest simulations,[22,23,25] the MD simulation corresponds to $R_e/a = 0.4$.

random variable dictated by the positions of entanglements, the rod explores areas of varying curvature as the tracer reptates along the tube. Thus, triblocks reptate on a nonuniform free energy surface, governed by the distribution of CM energies. This nonuniformity directly leads to slowed diffusion according to Zwanzig's formulation of diffusion on a rough potential.[24] While the CM energy distribution is narrow for $L \ll a$ because the tube is relatively straight on the length scale of short rods, this distribution widens for larger L because the tube's random curves of the primitive paths become significant at larger length scales. Thus, coil−rod−coils with longer rods reptate along rougher energy surfaces and hence diffuse more slowly.

The qualitative results of CM reptation can be calculated by treating the coil−rod−coil as a perturbation to existing coil reptation theory. For coil polymers, monomers are confined to the entanglement tube by a quadratic free energy potential, $U = k_BT(r/R_e)^2$, where r is the distance to the primitive path and R_e is the characteristic radius of the entanglement tube.[25−27] As a first approximation, it is assumed that this same potential also confines rod monomers and the presence of the rod does not affect the shape of the primitive path as defined by the coil polymer end blocks. Equating the confinement of rod and coil

dx.doi.org/10.1021/mz300127s | ACS Macro Lett. 2012, 1, 676−680

monomers is justified because the confining potential is generated by the homopolymer matrix and thus independent of the tracer. The validity of this approximation can be tested by calculating the rod's confining potential using the methodology of Zhou and Larson,[25] where the ends of all polymers are held fixed and the rod is allowed to explore its neighboring entanglements without reptating along the tube. The deviations of the rod's center of mass from the tube's centerline should follow a distribution related to its confining potential. This distribution precisely follows a cylindrically symmetric Gaussian function (Figure 3), indicating that the rod's center of mass is confined by a potential of the same quadratic form as coil monomers.

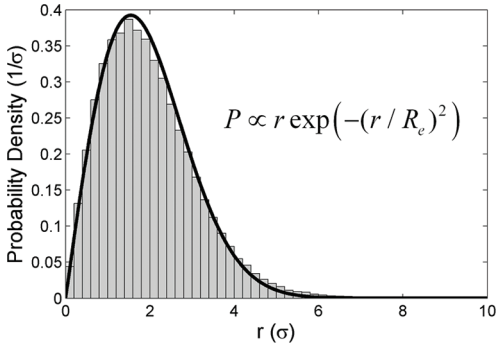

Figure 3. Probability distribution of the rod's center of mass deviation from its entanglement tube, which indicates that the rod is confined by a Gaussian potential. The data is averaged from 40 tracers at every 100τ over a total of $320\,000\tau$ time units. The tracers are coil−rod−coils with 300 total beads with a rod length of 16.

To estimate the effect of CM reptation on diffusion, the CM free energy distribution was calculated from an ensemble of 4000 entanglement tubes for a range of R_e/a and L/a. The primitive paths of these tubes were random wormlike chains with the persistence length $a/2$, resulting in random walk statistics with step size a. For each primitive path, the CM energy of the rod block was the ensemble average energy of all rod configurations at a given position. This energy was calculated by Metropolis Monte Carlo simulations, where the energy of a single rod configuration was the integral of the coil monomer's quadratic confining potential along the rod.[28] From the resulting distribution of 4000 CM energies, Zwanzig's theory was then used to calculate the ratio of diffusion on the nonuniform surface to a uniform surface, that is, the ratio of coil−rod−coil triblock copolymer to coil homopolymer diffusivity (Figure 2b).

Although the analytical CM theory does not quantitatively reproduce the results of MD simulation, it confirms the qualitative observations. Both simulation and theory illustrate that the coil−rod−coil triblocks nonintuitively diffuse slower than coil homopolymers, and both show that this slowing effect is independent of the size of the coil blocks. The CM theory illustrates that reptation on an increasingly rough free energy surface directly causes diffusion to slow down as the rod length approaches the entanglement tube diameter. In addition, CM reptation predicts that D/D_0 is independent of the coil block size because CM only occurs between the rod block and the surrounding matrix, so the slowing effect is only a function of L/a, in agreement with simulation results.

While CM reptation qualitatively explains diffusion in the short rod regime, the failure to quantitatively predict the MD results indicates the limited accuracy of the approximations for tube shape and confining potential. Additional research to determine the dependence of the entanglement radius R_e on rod length, the effect of the rod on tube shape, and the relationship between the center of mass confinement and the confinement of individual rod monomers is clearly important for calculating quantitative CM energy distributions and resulting predictions for diffusion. Nonetheless, the approximations utilized herein capture the physics of curvature mismatch.

In the large rod limit when $L \gg a$, reptation dynamics are sufficiently slow that other diffusion mechanisms become competitive with CM reptation. Direct MD simulation in this regime is difficult because enormous simulation boxes are required to maintain the dilute $\nu < L^{-3}$ condition. However, because the rod rotational relaxation ($\tau_r \sim L^5$ for rod tracers)[13,15] is much slower than reptation in this limit, the surrounding melt may be approximated as fixed obstacles on a cubic lattice. Although this approximation neglects the arrangement and mobility of the melt, it accurately preserves the underlying physics[29,30] at reasonable computational expense. Cubically arranged obstacles simplify the simulation while approximating the correct behavior, as both ordered and disordered obstacles severely hinder rotation for sufficiently long rods. 1600 tracers were simulated for diffusion measurements at various rod lengths and tube diameters, with a total degree of polymerization of 200 monomers (details in Supporting Information).

MD simulations in the large rod limit clearly show that triblock tracers diffuse more slowly as the coil fraction increases (Figure 4a). The exponential dependence is explained by the severely hindered rod rotation, such that diffusion of the rod is restricted to an extended region parallel to the rod's director (Figure 4a, inset). Although most configurations of the coil blocks extend outside this region, Fickian diffusion is possible for a fraction f of coil configurations that are confined to this extended region. Since blob scaling theories predict the free energy of confinement to one dimension scales as N_c/a^2, where a is the tube diameter,[31] the diffusivity of a triblock at constant total molecular weight scales as $D \sim \exp(-\nu N_c/a^2)$, where N_c is the coil size and ν is an order unity prefactor. This scaling is confirmed when the data is replotted against N_c/a^2 (Figure 4b) and is identical to the scaling for diffusion by arm retraction in star polymers.[32,33] This dynamic similarity of rod−coil block copolymers with star polymers is unexpected because the molecular architectures and mechanisms of diffusional slowing are quite different. For rod−coils, the rotationally hindered rod serves the same function as the branch point of star polymers. This correspondence is only satisfied in the long rod regime when a severe curvature mismatch effect prohibits overall reptation.

The crossover between the CM reptation and arm retraction regimes can be estimated using scaling analysis. The two mechanisms are dynamically competitive when the two predicted diffusivities are of the same order. In arm retraction, this diffusivity is $D \sim D_0^r \exp(-\nu N_c/a^2)$, where D_0^r is the diffusivity of a rod homopolymer of the same degree of polymerization. In CM reptation, this diffusivity is $D \sim D_0^c f(L/a)$, where D_0^c is the diffusivity of a coil homopolymer of the same degree of polymerization and f is a monotonically decreasing function of L/a. Since $f(L/a) \sim (D_0^r/D_0^c)\exp(-\nu N_c/a^2)$ at the crossover and both (D_0^r/D_0^c) and $\exp(-\nu N_c/a^2)$ decrease with the polymer degree of polymerization at constant

dx.doi.org/10.1021/mz300127s | ACS Macro Lett. 2012, 1, 676−680

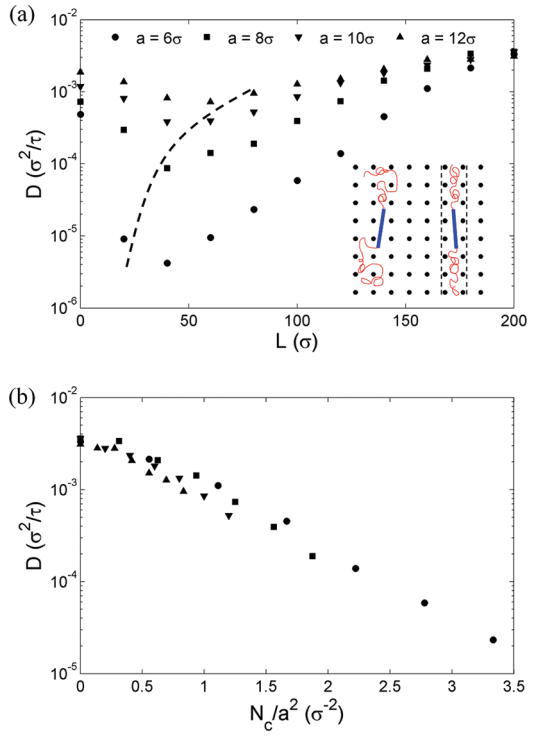

Figure 4. (a) Diffusivity as a function of rod length at various tube diameters in the fixed lattice MD simulation. There is a clear exponential dependence on rod length to the right of the dotted line, where the rods are too long to rotate around the fixed obstacles and the observed rotational relaxation time is infinite. The total degree of polymerization is 200, and the "tube diameter" a is the same as the unit spacing of the surrounding lattice. The inset illustrates chain configurations incapable (left) and capable (right) of Fickian diffusion due to rod diffusion restricted to being parallel to its director. (b) Data from (a) for $L \geq 80$ are replotted against N_c/a^2 and collapse onto a single curve, confirming theoretical predictions.

rod fraction, this analysis predicts that the crossover between the two regimes occurs at longer rod lengths for larger tracers.

Our investigations thus far have been limited to coil−rod−coil triblock copolymers, which are a convenient starting point since the shape of the entanglement tube is dictated by the disengagement of the two ends in the small rod regime. The common rod−coil diblock architecture[2] is more complex because of the potential for asymmetric disengagement of the rod and coil ends from the entanglement tube. The slowing effect associated with curvature mismatch is hypothesized to apply to the rod−coil diblock system; however, a thorough analysis of diblocks must additionally account for the asymmetric molecular structure.

In summary, MD simulations have demonstrated that entangled coil−rod−coil block copolymers diffuse more slowly than both rod and coil homopolymers of the same size. This dynamic arrest results from a mismatch between the characteristic curvatures of the rod and coil entanglement tubes. In the small rod limit, motion guided by the coil blocks is a reptation process with energy barriers from the presence of the rod. In the large rod limit, motion guided by the rod block is an arm retraction process from the presence of the coil. The molecular mechanisms presented here represent an important foundation for understanding the dynamics of other rod−coil molecular architectures such as rod−coil diblock copolymers, and they are an important step toward a broader understanding of dynamics in these increasingly important functional polymers.

■ ASSOCIATED CONTENT

Supporting Information

Simulation details in the small and large rod regimes and details for calculating curvature mismatch energies. This material is available free of charge via the Internet at http://pubs.acs.org.

■ AUTHOR INFORMATION

Corresponding Author

*E-mail: bdolsen@mit.edu.

Notes

The authors declare no competing financial interest.

■ ACKNOWLEDGMENTS

We thank T. A. Hatton for the use of computational resources, as well as R. Van Lehn and the NSF for Teragrid/XSEDE resources under Grant Nos. TG-DMR100077, TG-DMR110032, and TG-DMR110092. This research was supported by both the Chang fund of the MIT Research Support Committee and a DuPont fellowship. M.W. acknowledges funding through a NDSEG Fellowship.

■ REFERENCES

(1) Segalman, R. A.; McCulloch, B.; Kirmayer, S.; Urban, J. J. *Macromolecules* **2009**, *42* (23), 9205−9216.
(2) Olsen, B. D.; Segalman, R. A. *Mater. Sci. Eng. R* **2008**, *62* (2), 37−66.
(3) van Hest, J. C. M. *Polym. Rev.* **2007**, *47* (1), 63−92.
(4) Kohn, W. D.; Mant, C. T.; Hodges, R. S. *J. Biol. Chem.* **1997**, *272* (5), 2583−2586.
(5) Chen, J. T.; Thomas, E. L.; Ober, C. K.; Mao, G. P. *Science* **1996**, *273* (5273), 343−346.
(6) Olsen, B. D.; Shah, M.; Ganesan, V.; Segalman, R. A. *Macromolecules* **2008**, *41* (18), 6809−6817.
(7) Lee, M.; Cho, B. K.; Zin, W. C. *Chem. Rev.* **2001**, *101* (12), 3869−3892.
(8) Gopalan, P.; Zhang, Y. M.; Li, X. F.; Wiesner, U.; Ober, C. K. *Macromolecules* **2003**, *36* (9), 3357−3364.
(9) Olsen, B. D.; Teclemariam, N. P.; Muller, S. J.; Segalman, R. A. *Soft Matter* **2009**, *5* (12), 2453−2462.
(10) Yoda, R.; Hirokawa, Y.; Hayashi, T. *Eur. Polym. J.* **1994**, *30* (12), 1397−1401.
(11) Borsali, R.; Lecommandoux, S.; Pecora, R.; Benoit, H. *Macromolecules* **2001**, *34* (12), 4229−4234.
(12) de Gennes, P. G. *J. Chem. Phys.* **1971**, *55* (2), 572−579.
(13) Doi, M.; Edwards, S. F. *The Theory of Polymer Dynamics*; Clarendon: Oxford, 1986.
(14) Tao, H.; Lodge, T. P.; von Meerwall, E. D. *Macromolecules* **2000**, *33* (5), 1747−1758.
(15) Doi, M.; Edwards, S. F. *J. Chem. Soc., Faraday Trans. II* **1978**, *74*, 918−932.
(16) Tracy, M. A.; Pecora, R. *Annu. Rev. Phys. Chem.* **1992**, *43*, 525−557.
(17) Bu, Z.; Russo, P. S.; Tipton, D. L.; Negulescu, I. I. *Macromolecules* **1994**, *27* (23), 6871−6882.
(18) Maguire, J. F.; McTague, J. P.; Rondelez, F. *Phys. Rev. Lett.* **1980**, *45* (23), 1891−1894.
(19) Jin, L. Y.; Bae, J.; Ryu, J. H.; Lee, M. *Angew. Chem., Int. Ed.* **2006**, *45* (4), 650−653.
(20) Kremer, K.; Grest, G. S. *J. Chem. Phys.* **1990**, *92* (8), 5057−5086.
(21) Hoy, R. S.; Foteinopoulou, K.; Kroger, M. *Phys. Rev. E* **2009**, *80* (3), 031803.

(22) Everaers, R.; Sukumaran, S. K.; Grest, G. S.; Svaneborg, C.; Sivasubramanian, A.; Kremer, K. *Science* **2004**, *303* (5659), 823−826.
(23) Sukumaran, S. K.; Grest, G. S.; Kremer, K.; Everaers, R. *J. Polym. Sci., Part B* **2005**, *43* (8), 917−933.
(24) Zwanzig, R. *Proc. Natl. Acad. Sci. U.S.A.* **1988**, *85* (7), 2029−2030.
(25) Zhou, Q.; Larson, R. G. *Macromolecules* **2006**, *39* (19), 6737−6743.
(26) Robertson, R. M.; Smith, D. E. *Phys. Rev. Lett.* **2007**, *99* (12), 126001.
(27) Wang, B.; Guan, J.; Anthony, S. M.; Bae, S. C.; Schweizer, K. S.; Granick, S. *Phys. Rev. Lett.* **2010**, *104* (11), 118301.
(28) Sample curvature mismatch energies and distributions can be found in the Supporting Information.
(29) Evans, K. E.; Edwards, S. F. *J. Chem. Soc., Faraday Trans. II* **1981**, *77*, 1891−1912.
(30) Rubinstein, M. *Phys. Rev. Lett.* **1987**, *59* (17), 1946−1949.
(31) Rubinstein, M.; Colby, R. H. *Polymer Physics*; Oxford University Press: New York, 2003.
(32) Doi, M.; Kuzuu, N. Y. *J. Polym. Sci. C* **1980**, *18* (12), 775−780.
(33) Pearson, D. S.; Helfand, E. *Macromolecules* **1984**, *17* (4), 888−895.